Charge-Transfer-Type Fluorescence of 4-(1*H*-Pyrrol-1-yl)benzonitrile (PBN) and *N*-Phenylpyrrole (PP) in Cryogenic Matrixes: Evidence for Direct Excitation of the CT Band

D. Schweke, H. Baumgarten, and Y. Haas*

Department of Physical Chemistry and the Farkas Center for Light Induced Processes, The Hebrew University of Jerusalem, Jerusalem, Israel

Wolfgang Rettig

Humboldt University of Berlin, Brook-Taylor-Strasse 2, D-12489 Berlin, Germany

Bernhard Dick

Lehrstuhl für Physikalische Chemie, Universität Regensburg, Regensburg, Germany

Received: September 26, 2004; In Final Form: October 22, 2004

The fluorescence spectrum of PBN in a neat argon matrix is excitation-wavelength-dependent: at short excitation wavelengths, it consists of dual emission assigned to a charge-transfer (CT) state and a much weaker band assigned to the locally excited (LE) state. The CT emission is broad and almost completely devoid of vibrational structure, whereas the LE band is characterized by vibrationally resolved emission. At long excitation wavelengths, only CT emission is observed, indicating that the CT state is populated directly by light absorption and not via the LE state. Comparison with jet-cooled spectra of the bare molecule allows the unambiguous assignment of the LE spectrum and the location of the 0,0 band. The matrix LE emission spectrum is blue-shifted with respect to that of the gas phase, showing that the dipole moment of the LE state is smaller than that of the ground state. The fluorescence spectrum of PBN in an argon matrix does not change appreciably when acetonitrile (AN) is added to the matrix, in contrast to the case of *N*-phenylpyrrol (PP) (Schweke, D.; Haas, Y. *J. Phys. Chem. A* **2003**, *107*, 9554), for which addition of AN results in the appearance of two well separated emission bands. The different photophysical behaviors of PP and PBN in an argon matrix (and in supersonic jets) are analyzed by a simple model that considers the restriction of large-amplitude motions in the matrix. The implications of these low-temperature studies for understanding the properties of these systems in liquid solution are discussed.

I. Introduction

N-Phenylpyrrol (PP) and its derivative 4-(1*H*-pyrrol-1-yl)-benzonitrile (abbreviated PBN) belong to a group of molecules exhibiting dual fluorescence in solution.[1] Because of the much stronger electron-attracting power of the benzonitrile moiety compared to the phenyl one, their fluorescence spectra display different solvent dependence. In nonpolar solvents, the emission spectrum of PP is largely due to a locally excited (LE) state related to the 1^1B_{2u} state of benzene, labeled hereafter as the B state,[2,3] whereas in polar solvents, dual emission is observed, the red-shifted band being assigned to a charge-transfer (CT) state, derived from the A state.[4] The ground state will be denoted as the X state. In contrast, the emission spectrum of PBN in nonpolar solvents such as cyclohexane is mostly due to the CT state (the B → X emission band appears as a shoulder),[5,6] whereas in a polar solvent such as acetonitrile, the emission is strongly red-shifted and is due almost entirely to a CT state (i.e., an A → X transition).[6] We have recently studied the fluorescence of both molecules in a supersonic jet[7,8] and of PP in cryogenic matrixes.[9] These studies were carried out at very low temperatures, in which only the lowest vibrational levels of the ground electronic state are populated. They allow accurate determination of the 0,0 bands of the isolated molecule in the gas phase. Both molecules show only LE-type fluorescence in a supersonic jet, i.e., when isolated from any interaction with the surroundings. Thus, the CT state is higher in energy than the LE one for both molecules under these conditions. Moreover, excitation to high vibrational levels of the LE state does not lead to population of the CT state. When the polar molecule acetonitrile (AN) is added to the expanding jet, it forms clusters with the pyrrol derivatives; the emission from these clusters is dramatically different for the two molecules: $PBN(AN)_n$ clusters exhibit dual fluorescence (for $n \geq 4$), whereas for $PP(AN)_n$, only a single electronic state (the LE state) emits for any number of AN molecules.[8] The second, red-shifted band (observed for $PBN/AN_{n\geq 4}$ clusters) was assigned to a charge-transfer (CT) state, on the basis of the comparison with liquid solution spectra. In a neat argon matrix, PP shows LE emission only, but when AN is added, fluorescence emissions due to both LE and CT states are observed as separate bands.[9]

In this paper, we report experimental results obtained for PBN in an argon matrix, neat and with AN added. In addition spectra obtained in some other cryogenic matrixes are reported. The data analysis is aided by comparison with other bulk environ-

* To whom correspondence should be addressed. E-mail: yehuda@chem.ch.huji.ac.il.

10.1021/jp045629t CCC: $30.25
Published on Web 01/05/2005

ments and also with the spectra obtained for clusters in a cold jet. Simulations of the structures of PP/AN and PBN/AN clusters help to account for the observed differences between the two pyrrol derivatives.

II. Experimental and Computational Methods

II.1. UV Spectroscopy. PBN was prepared and purified as previously described.[10] Samples were deposited on a BaF_2 or sapphire window, held at the tip of an APD 202 closed-cycle helium cryostat. PBN vapor was premixed with the host gas (99.999%, typical guest/host ratio of 1:10000) and in some experiments with AN (Aldrich, 99.5%) vapor in a stainless steel feed line and deposited at 25 K through a needle valve at a rate of about 3 mmol/h. Fluorescence was excited using either a dye laser (Lambda Physik FL3002) pumped by an excimer laser (Lambda Physik EMG101MSC) or a picosecond laser (Continuum Leopard at 266 nm, 20 ps pulse width). Emission spectra were measured with 10−40 cm^{-1} resolution using a Spex model 1702/4 0.75-m spectrometer. Detection was done with a Hamamatsu R928 photomultiplier tube for the time-resolved measurements and with an EMI 9558 for the steady-state emission spectra. The resulting signal was digitized by a Tektronix model 2430 oscilloscope and processed by a Pentium IV personal computer. Decay times were measured by feeding the PM current into a 50Ω terminator and fitting the resulting decay curve to an exponential function. Extensive signal averaging was employed when necessary until an acceptable S/N ratio was obtained.

II.2. Computational Methodology. For the structural calculations, we approximated the interaction energy between two molecules A and B by a sum of pair potentials between the atoms *a* and *b* on each molecule

$$V_{\text{int}} = \sum_{A<B} V_{\text{AB}}$$
$$V_{\text{AB}} = \sum_{a\in A}\sum_{b\in B} \frac{1}{4\pi\epsilon_0}\frac{q_a q_b e^2}{R_{ab}} + 4\epsilon_{ab}\left[\left(\frac{\sigma_{ab}}{R_{ab}}\right)^{12} - \left(\frac{\sigma_{ab}}{R_{ab}}\right)^{6}\right] \quad (1)$$

where R_{ab} is the distance between atoms *a* and *b*, ϵ_{ab} is the well depth of the Lennard-Jones (LJ) interaction potential between the two atoms, σ_{ab} is the contact distance at which the LJ potential equals zero, and q_i is the electronic charge on atom *i*. ϵ_{ab} and σ_{ab} are given by the usual combination rules[11]

$$\epsilon_{ab} = \sqrt{\epsilon_{aa}\epsilon_{bb}}$$
$$\sigma_{ab} = \frac{1}{2}(\sigma_{aa} + \sigma_{bb}) \quad (2)$$

The potential parameters for PP and PBN were taken from OPLS (optimum parameters for liquid simulations) of pyrrole,[12] benzene,[13] and benzonitrile.[13] For AN, Bohm parameters[14] were used. The values used for these parameters are presented in the Supporting Information. During cluster optimization, the molecules PP, PBN, and AN were considered rigid. Therefore, the interaction energy between atoms on the same molecule is constant and was not included in eq 1. The geometry of a cluster is thus defined by one distance vector and one set of Euler angles for each of the AN molecules that describe the position of this ligand in the reference frame defined by the PP or the PBN molecule. The geometries for the ground-state PP and PBN molecules were obtained from DFT calculations (B3LYP functional, cc-pVDZ basis set), whereas those for the CT state were calculated at the CAS (12,12) level.[15] ESP (electrostatic potential) charges[16] were calculated for the equilibrium geometry of each electronic state and used in eq 1. For each system, 200 randomly generated starting geometries were optimized using either the Simplex algorithm[17] or two different algorithms developed by Powell[18,19] and implemented by available codes.[20] Two (or three) local minima were found for PP (or PBN) 1:1 clusters with AN.[21] The lowest energy minima for each pair (which are the relevant ones in the experimental conditions since local annealing occurs during matrix deposition) are reported. More details on the calculation will be reported separately.[21]

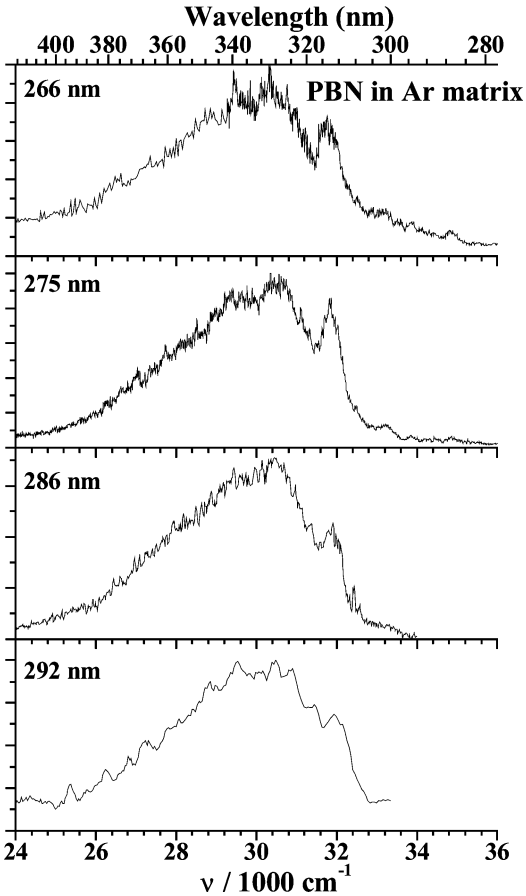

Figure 1. Emission spectra in argon obtained upon excitation at different wavelengths. The top spectrum has been measured at 13 K, the others at 25 K.

III. Results

Emission spectra of PBN in argon (~1:10000) excited at several different wavelengths are shown in Figure 1. The overall shape of the spectra appears to be rather insensitive to the excitation wavelength, but closer inspection reveals some variations. A vibrational structure is observed in the blue edge of the first two emission spectra, for which the excitation wavelengths (266 or 275 nm) are short enough. Figure 2 shows the peaks and relatively narrow bands in more detail. A prominent band around 32000 cm^{-1} that is much broader than the weaker bands of higher frequency (a few hundred wavenumbers) might also be due to a vibronic band, but its nature appears to be different. The expanded view of this region, shown in Figure 2, is compared with the spectrum of PBN in a supersonic jet. An excitation spectrum monitored at 343 nm and run between 285 and 293 nm showed nearly monotonic decreasing signal intensity for longer wavelengths and was broad and almost structureless. The poor S/N ratio did not permit a

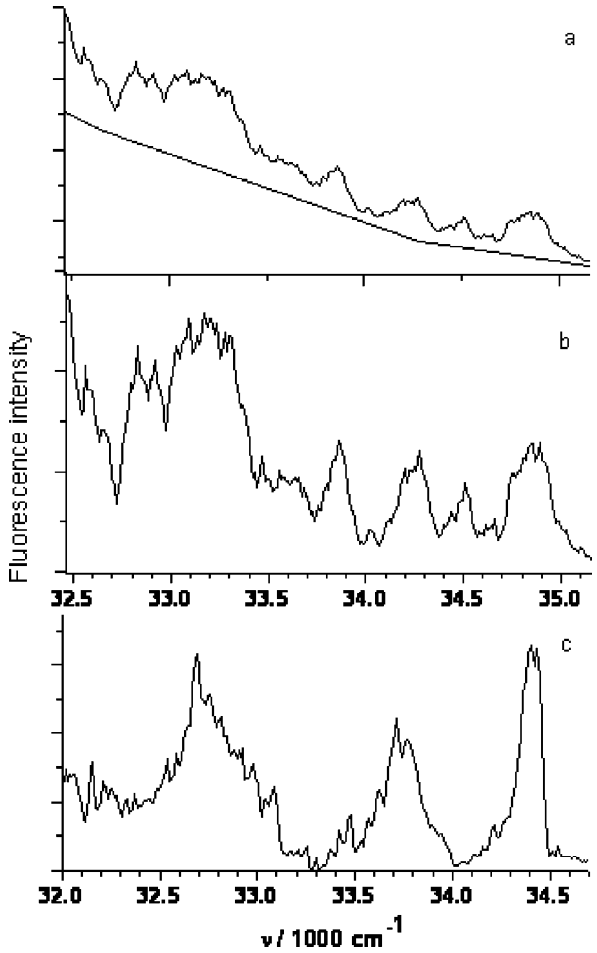

Figure 2. (a) Expanded view of the structured part of the emission spectrum of PBN in an argon matrix, excited at 266 nm. (b) Same spectrum after subtraction of the broad band; depicted as a dotted line in the top figure. Its shape was determined by extrapolation of the strong emission band assigned to the CT band shown in the figure. (c) Emission spectrum of PBN recorded in the jet upon excitation at the 0−0 band.

proper analysis, except for noting that beyond 293 nm, the signal was not discernible above the noise.

Emission spectra obtained in a N_2 matrix at 25 K yielded similar results. Some numerical data of the spectra of PBN in an argon matrix are collected in Table 1. The excited-state lifetimes measured for several emission wavelengths are listed in Table 2. The differences noted between the lifetimes obtained for the red and blue parts of the spectrum are not large, but are beyond the estimated error limit.

Codeposition of PP and AN in an argon matrix resulted in a dramatic spectral change compared with neat PP in the same matrix: a new band appeared that was strongly red-shifted and could be assigned to a CT transition.[9] The effect of AN addition to a PBN/Ar matrix appears to be much less pronounced. The general form of the spectrum is hardly changed, but closer inspection shows that the fine structure at the blue edge has disappeared. The effects of the excitation wavelength and AN concentration on the recorded spectrum were also checked (Figure 3). The spectrum is slightly shifted to the red upon excitation at longer wavelengths; increasing the concentration of AN leads to the appearance of a shoulder at the red edge of the spectrum.

The emission spectra of PBN were also recorded in xenon (at 40 K) and CO_2 (at 20 K) matrixes. Both xenon and carbon dioxide are more polarizable than argon: the average polarizabilities of argon, CO_2, and xenon are 1.63, 2.65, and 4.01 Å^3, respectively. Figure 4 reports the emission spectra recorded in these different matrixes. It is seen that, as the matrix becomes more polarizable, the spectrum shifts to the red. The emission spectrum in xenon is considerably broader than that in argon or CO_2. It is noted that, in xenon, the cavities containing the trapped species are larger.

TABLE 1: Frequencies and Widths (cm^{-1}) of the Main Vibronic Peaks of the Fluorescence Bands in the Spectrum of PBN in an Argon Matrix

number[a]	frequency (cm^{-1})	height[b] (arbitrary units)	width[c] (cm^{-1})
1	35460	4.5	220
2	34870	19.1	220
3	34510	10.8	100
4	34220	14.1	160
5	33860	17.0	130
6	33600	33.3	–
7	33190	36.2	420
8	32920	27.9	220
9	32830	30.4	
10	32560	26.6	240
11	32470	38.3	
12	32400	33.3	
13	32250	38.3	550
14	32100	50.3	
15	31890	100	
16	31740	85.8	
17	31550	58.2	
18	31430	26.4	

[a] For a complete listing of the bands, please see Figure S1 in the Supporting Information. [b] Intensity at the maximum of the peak. [c] Width of the band (fwhm); the measured widths of most bands indicate that they actually are composite ones, including several neighboring transitions that are not sufficiently separated. The widths listed are of the composite band, which in some cases are partly resolved (e.g., bands 10 and 11).

TABLE 2: Fluorescence Lifetimes (ns) Measured in an Argon Matrix[a] upon Excitation at 266 nm with a Picosecond Laser

		τ_f (ns)	
λ_{em} (nm)	ν_{em} (cm^{-1})	13 K	25 K
300	33333	9.9	10.0
307	32570	9.9	10.2
340	29410	13.6	14.1
385	25970	13.8	13.2
400	25000	13.0	–

[a] Estimated errors are ±0.5 ns.

IV. Discussion

IV.1. Nature of the Emitting States of PBN in a Neat Argon Matrix. Bare jet-cooled PBN molecules emit only from the LE state, whereas clusters with AN (with more than four AN molecules) have recently been shown to exhibit CT fluorescence in a supersonic jet.[6] In solution, the dominant emission is from the CT state even in a nonpolar solvent.[5,6] Therefore, it appears that some insight into the nature of the emission spectrum of PBN in an argon matrix can be gained by comparing it to spectra obtained in other media. Figure 5 shows the spectra in cyclohexane (CH) at room temperature and in an argon matrix. The close similarity of the spectra and the fact that these two solvents have similar dielectric constants (CH, 2.02; Ar, 1.56) suggests that the dominant part of the spectrum in an argon matrix is due to the CT state.

This assignment for PBN in an argon matrix is supported by comparison with the jet spectra. Figure 6 shows a comparison

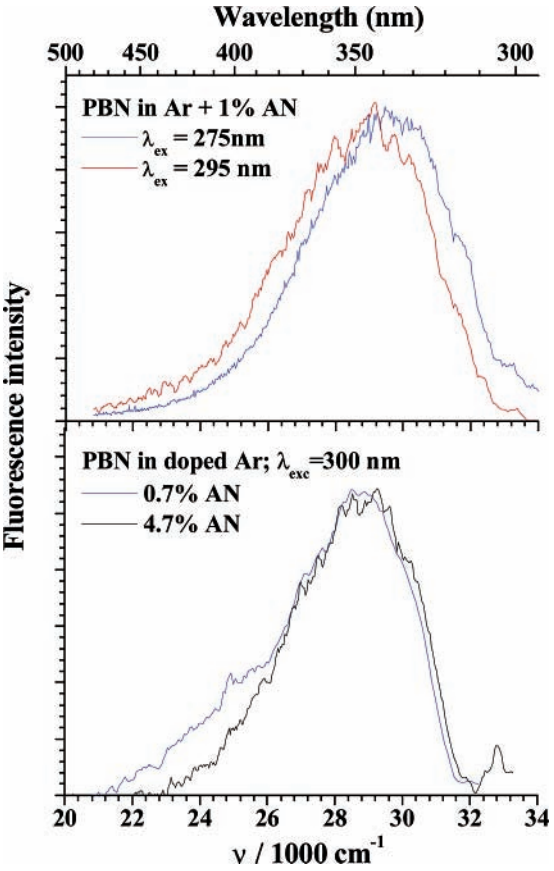

Figure 3. Emission spectra of PBN in an argon matrix to which AN was added at different excitation wavelengths and concentrations of AN. The PBN/argon ratio was about 1:10000.

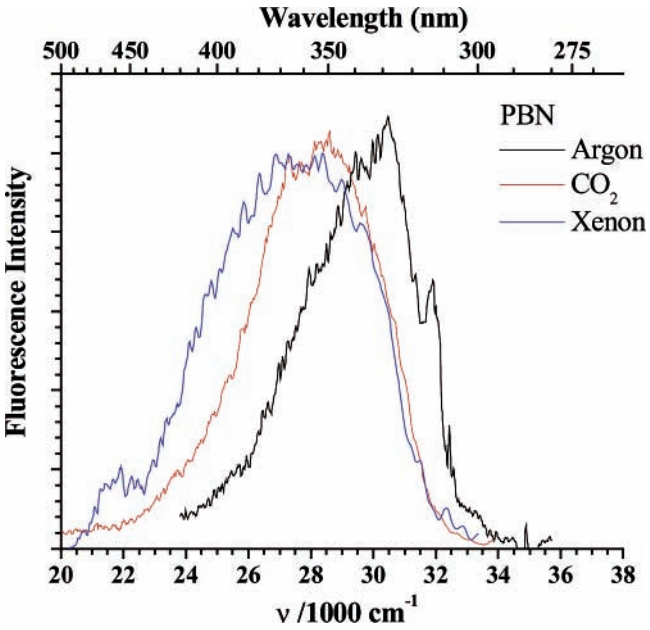

Figure 4. Emission spectra of PBN recorded in matrixes of different composition: argon (T_{dep} = 25 K), xenon (T_{dep} = 40 K), and CO_2 (T_{dep} = 20 K). All spectra were measured at the deposition temperatures and excited at 285 nm.

of the jet spectra of isolated PP and PBN molecules with the corresponding argon matrix spectra. It is clear that, whereas the PP spectra are quite similar in the two environments [apart from a small (445 cm^{-1}) *red* shift of the matrix spectrum with respect to the jet one], the PBN spectrum in an argon matrix is much broader than that in the jet. The "extra" part extends to the red

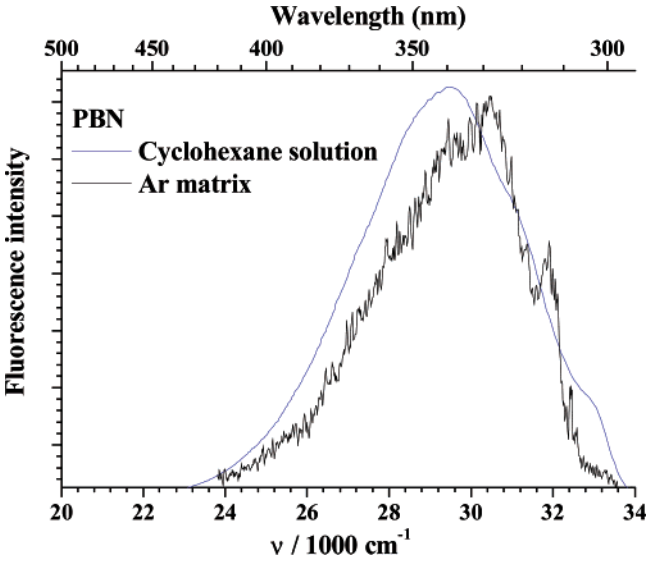

Figure 5. Comparison of PBN emission spectra in cyclohexane and in an argon matrix. Blue: Emission spectrum in cyclohexane solution at room temperature, excitation at 280 nm. Black: Emission spectrum in argon matrix at 25 K, excitation at 286 nm.

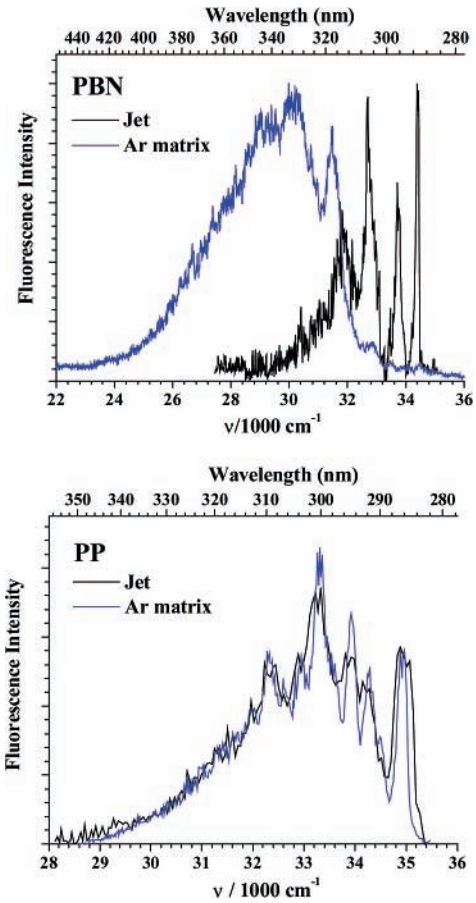

Figure 6. Comparison of the jet emission spectra (black) with those of the matrix-isolated molecules (blue). The jet spectra have been shifted so that the jet 0−0 band matches the 0−0 band recorded in the argon matrix (the shifts with respect to the matrix spectra are −445 and +446 cm^{-1} for PP and PBN, respectively (left, PBN; right, PP). Note the different widths of the spectra.

and can be explained by assuming that the CT state contributes significantly to the spectrum.

Figure 7 shows in detail a similar comparison between the emission spectra of PBN in the jet and in an argon matrix (Table

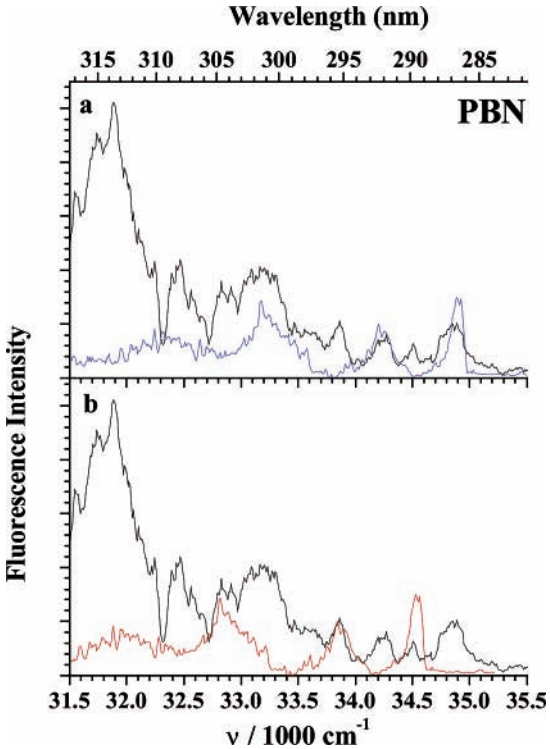

Figure 7. Comparison between the jet spectrum (color) and the blue part of the argon matrix spectrum (black). The jet spectrum has been shifted to show the overlap of the matrix spectrum with the jet one. At least two series of vibrational bands that fit the jet spectrum are found in the argon matrix; they might be due to two different trapping sites.

3 lists the numerical values).[22] Although a vibrational structure is clearly observable, with a much better resolution than recorded in room-temperature solution spectra, the low resolution and relatively poor S/N ratio do not allow an accurate vibronic assignment of the spectra. In fact, each of the three broad bands shown is a poorly resolved superposition of several vibrational bands. Nevertheless, the vibrationally resolved part of the matrix spectrum is seen to nicely overlap the jet spectrum. Two series of bands can be discerned, both blue-shifted with respect to the gas-phase jet spectrum: one with a matrix blue shift of about 446 cm^{-1} (Figure 7a and Table 3) and the other with a blue shift of about 86 cm^{-1} (Figure 7b and Table 3). They are tentatively assigned to two different trapping sites of PBN in an argon matrix.

The two vibrational bands around 31900 and 32470 cm^{-1} are evidently not part of the two progressions listed in Table 3: These peaks are much broader and have different substructure. We tentatively assign them to a charge-transfer band whose nature is discussed below. The fact that, in the jet spectrum, the X−B transition appears at lower energy than the matrix one indicates that the excited state is less polar in this case than the ground state. For PBN, the dipole moment of the LE B state was calculated to be equal to[15] or higher than[23] that of the ground state. Experimentally, based on liquid solution spectra,[5] the dipole moments appeared to be of the same order of magnitude.

The fluorescence decay times (Table 2) support the assignment of the emission spectrum to two different states. As clearly seen from Figures 1 and 2, the emission at the vibronic bands is superimposed on a broad background that is probably due to a CT band. The intensity of the vibronic bands assigned to the LE state is much smaller than that of the main CT band, so that even a small contribution of the CT band in the shorter-wavelength region cannot be neglected. The shorter decay times (9.5 ± 1 ns) measured for these discrete bands compared to the broad CT band (13.5 ± 1 ns) are thus probably due to an average between the true LE lifetimes and the CT lifetime. The measured value is therefore an upper limit of the true decay time of PBN in an argon matrix. In the jet, the decay time of the CT state of PBN/AN clusters was about 26 ns[8] (corresponding to a decay rate constant $k^{CT}_{PBN/AN} = 3.8 \times 10^7\ s^{-1}$), whereas the LE state had a decay time of about 12 ns ($k^{LE}_{PBN/AN} = 8.3 \times 10^7\ s^{-1}$). In an argon matrix (Table 2), we measured 13.5 ns for $\lambda_{em} \geq 340$ nm ($k^{CT}_{PBN} = 7.4 \times 10^7\ s^{-1}$) and at most 9 ns ($k^{LE}_{PBN/Ar} \geq 11 \times 10^7\ s^{-1}$) for the blue part of the spectrum. The larger rate constants in the argon matrix indicate that an additional nonradiative process is operative for both states with a rate constant of about (3 ± 1) × $10^7\ s^{-1}$, possibly due to intersystem crossing (ISC) to a triplet state. Triplet yields have not yet been reported for PBN, but data available for DMABN and some derivatives[1] can help to determine order of magnitude values. In solution, the yields are quite high (50−80%), reflecting an intersystem rate constant of the order of $10^8\ s^{-1}$ that might be temperature-dependent.[24] Because intersystem crossing is expected to be more efficient in the presence of argon than in organic solvents not substituted by heavy atoms, the derived rate constant appears reasonable.

IV.2. Energy Levels of PBN in an Argon Matrix: Direct Excitation of the CT State in an Argon Matrix. From Table 3, the origins of the transitions to the 1^1B (LE) state in the two trapping sites of PBN in an argon matrix are at 34510 and 34870 cm^{-1}. If the assignment is correct and if one assumes that population of excited vibrational levels is negligible in the argon matrix at 25 K, excitation of PBN at wavelengths longer than 290 nm (34480 cm^{-1}) cannot populate the LE state. The fact that fluorescence is observed in PBN-doped argon matrixes upon excitation in the range 290−295 nm (see Figure 4) *therefore means that excitation at these wavelengths must be directly to the CT state.* (A hot band populating the vibrationless state of the 1^1B state would require population of a ground-state vibrational level of 600 cm^{-1}). In liquid solution, the current consensus is that initial excitation is to the B (LE) state, which is much more likely to be populated because of Franck−Condon (FC) considerations. This view is based, among other pieces of evidence, on real-time measurements of the rise time of the fluorescence of PP[25] and similar molecules.[26] It was found that, whereas the LE emission arising from the B state is formed instantaneously, the CT emission from the A state rises more slowly, with a rate constant that matches the decay rate constant of the B state. In the case of PBN in a polar solvent, the rate of formation of the CT emission band is very large ($>10^{12}\ s^{-1}$).[25] Such large values could be due to the solvent reorganization process following the transition from a nonpolar state to a polar one. The standard model[1,25] considers a thermal equilibrium between the LE and CT states that are separated by a small barrier. The data presented here show that, in some cases, direct excitation of the CT state is possible. The thermal barrier might be due partly to the reorganization of the solvent around the solvated molecule.

Under ambient room-temperature conditions, transitions from vibrationally excited states of the ground state ("hot" bands) can overlap and mask weaker transitions from the zero-point energy level to the CT state. An advantage of the matrix work is that the temperature (25 K) is low enough to exclude most hot bands. This is demonstrated by calculating the relative population of a vibrational state lying at 350 cm^{-1} (1 kcal/mol) with that of the ZPE (zero point energy) state. At 25 K it is 1:(2×10^9), i.e., negligibly small, whereas at room temperature (300 K), the ratio is 1:5. Thus, the LE state is likely to be

TABLE 3: Band Positions (cm^{-1}) of the Three Main Vibronic Transition of PBN LE Fluorescence in Various Environments

jet[a]			Ar(I)			Ar(II)			N_2		
matrix shift			446			86			296		
band	ν (cm^{-1})	$\Delta\nu$ (cm^{-1})	band	ν (cm^{-1})	$\Delta\nu$ (cm^{-1})	band	ν (cm^{-1})	$\Delta\nu$ (cm^{-1})	band	ν (cm^{-1})	$\Delta\nu$ (cm^{-1})
0,0	34424	0	2	34870	0	3	34510	0	N_2 (1)	34720	0
first	33739	−685	4	34220	−650	5	33860	−650	N_2 (2)	34100	−620
second	32714	−1710	7	33190	−1680	9	32830	−1680	N_2 (3)	33030	−1690

[a] Reference 8. [b] Enumeration of bands from Table 1.

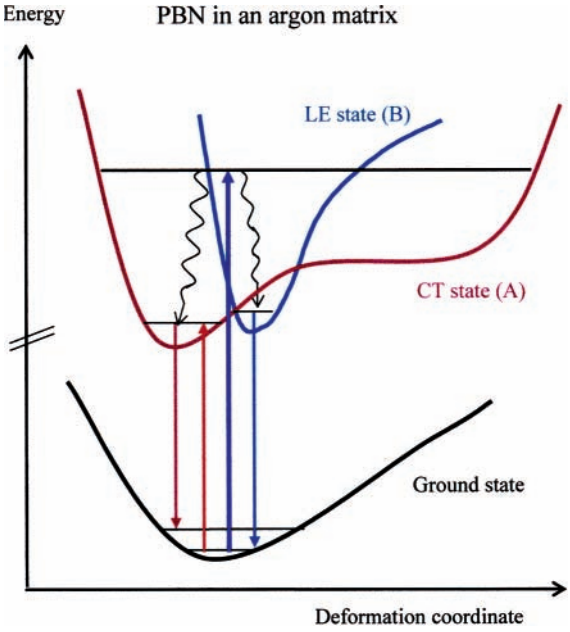

Figure 8. Schematic energy level diagram of PBN in an argon matrix as a function of the deformation coordinate leading from the LE geometry to the CT one (mainly quinoidization and torsion). The B state (LE, green curve) has an equilibrium geometry similar to that of the ground state. Two forms of the A (CT, violet curve) state are considered, Q and AQ, having minima in the gas phase at torsion angles 0° and 90°, respectively. The global minimum of the CT state is lower in energy than that of the LE state; it can be excited directly from the ground state at a relatively long wavelength (red arrow) leading to CT state emission only (violet arrow). At shorter wavelengths, excitation (blue arrow) followed by vibrational relaxation (wavy lines) leads to population of the minima of the two states (CT and LE) and to dual emission.

preferentially excited at room temperature, even if the CT state is lower in energy, because of more favorable FC factors. Yet, it is also possible that some direct excitation of CT occurs at higher temperatures.

The absence of any vibrational structure in the blue part of the CT emission spectrum is probably due to matrix phonon effects combined with small differences between several trapping sites. Franck−Condon transitions from the ZPE of the CT state are mainly to higher levels of the ground state (as is also observed in PBN/AN clusters in the jet[8]).

Figure 8 shows a schematic energy level diagram that is compatible with the matrix data. This diagram is based on a model proposed some time ago[15] for the charge-transfer state. There are two main models for the CT state: one contends that the benzene and pyrrolo rings are perpendicular to each other (twisted intramolecular charge transfer, TICT[27]), the other that the CT state is planar (planar intramolecular charge transfer, PICT[28]). In the Zilberg−Haas[15] model, both options were shown to be possible on the A-state potential surface that was calculated to have two minima, one planar and the other with a perpendicular (twisted) structure. The planar minimum has a quinoid structure, i.e., shortened central bonds of the benzene ring and a short $C-N_{pyrrol}$ bond, and is termed the Q form. The twisted one has an anti-quinoid structure, with lengthened central benzene bonds and $C-N_{pyrrol}$ bond, and is labeled as the AQ form. Both minima are on the same potential surface, the first electronically excited A state. In the isolated molecule, the planar structure (Q form) is lower in energy, but has a smaller dipole moment. The schematic energy diagram in Figure 8 is drawn as a one-dimensional cut along the deformation coordinate that includes all the structural changes undergone by the molecule during electronic relaxation, mainly quinoidization and twist. Two minima are drawn on the CT potential energy curve, one of them corresponding to the Q form and the second to the AQ form. Our data do not permit the assignment of the spectrum to one or the other. Molecular dynamics simulations of the trapping sites will be discussed extensively in a separate paper. They indicate that, because the geometry of the Q form is comparable to that of the ground state whereas the AQ form is more distorted, the CT state that emits in argon is likely to have the Q form. This potential energy diagram is compatible with recent ultrafast experiments by Fuss and co-workers.[29]

For the purpose of the present analysis, the main point is that the global minimum on the A-state surface (violet curve) in the argon matrix is lower than that of the B state (green) and the two curves cross at one or more points. Absorption at short wavelengths (blue arrow) populates both states; vibrational relaxation (wavy arrows) populates the low-lying vibrational levels, and dual emission is observed. Absorption at longer wavelengths (violet arrow) can populate only the CT state, leading to emission that is exclusively of CT character. The red shift of the CT emission with respect to the LE one is readily explained by this diagram. The real situation might be even more complex. Quantum chemical calculations[23] indicate that a state with B symmetry also has a CT character and might be considerably stabilized in a polar solvent. At this point, we cannot establish its contribution, but our data can be interpreted as suggesting that it also has an emitting minimum. As seen from Figures 1, 2, and 7, at least two resolved vibronic bands (centered at 31900 and 32470 cm^{-1}, Table 1) cannot be assigned to one of the two progressions due to the $1^1A\ (S_0)-1^1B$ (LE) transition. A possible assignment of these vibrational bands appearing in the spectrum is that they are due to this second CT state proposed by the calculations of ref 23.

IV.3. Effect of Added AN on the Emitting States of PBN in an Argon Matrix. The emission spectrum of PBN in AN clusters showed distinct dual emission: the CT band exhibited a notable red shift with respect to the LE spectrum.[8] In fact, the CT part of the spectrum was very similar to the spectrum recorded in neat AN, which is entirely due to the CT state. As shown in Figure 3, addition of AN to the argon matrix had only a minor effect on the spectral shift of the emission spectrum. This is in sharp contrast to the effect of added AN on the spectrum of PP in an argon matrix: in that case, a well-separated band due to CT emission was observed.[9] A qualitative model for these observations can be formulated considering the main

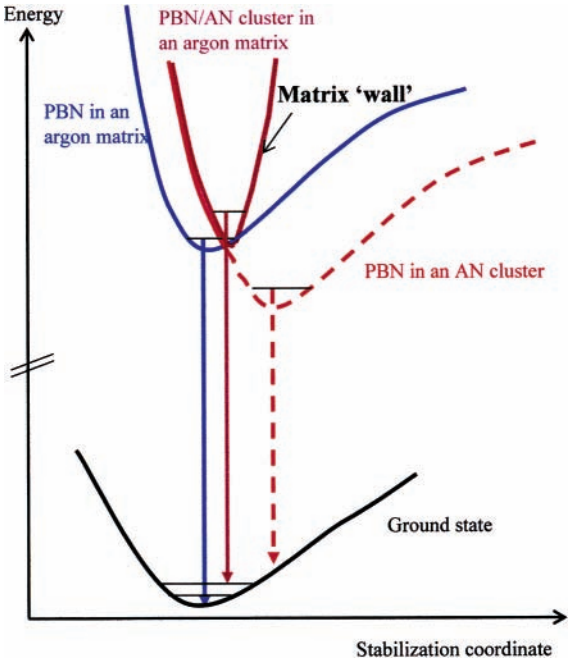

Figure 9. Schematic presentation of the energy level diagram of PBN in an argon matrix and in an AN-doped argon matrix as a function of the coordinate leading to the stabilization of the CT state. For clarity only one minimum is shown for the CT state and the LE potential curve was omitted. The ground state in shown in black, the CT states in different milieus in color. The blue curve depicts the energy of the CT state in neat argon; the red one, the expected curve in the presence of AN assuming complete structural optimization. The violet curve shows the effect of the matrix, i.e., the barrier it creates leads to an effective potential that shifts the emission spectrum (violet arrow) to the blue compared to the expected spectrum under full relaxation conditions (red arrow).

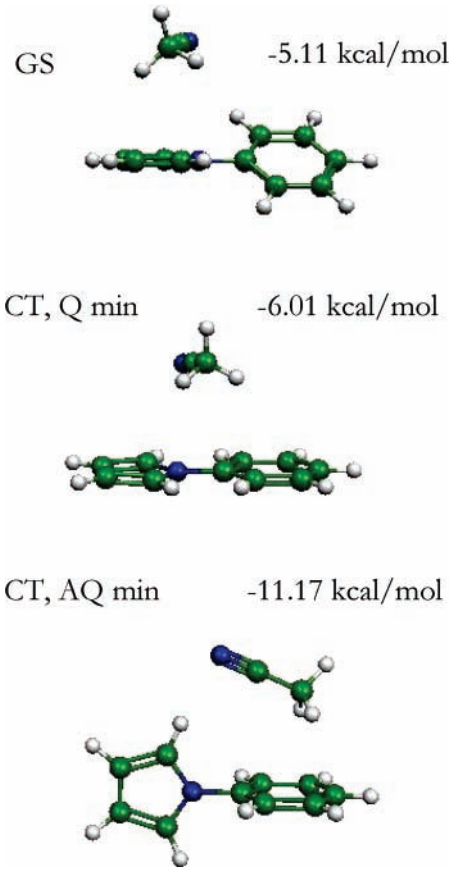

Figure 10. Calculated equilibrium structures of the most stable 1:1 PP/AN clusters in the ground state and in the two CT excited states. The energies signify stabilization with respect to the separated molecules.

difference between an argon matrix on one hand and a cluster and liquid solution on the other. In an argon matrix, large-amplitude motions are prohibited to a large extent, whereas in a cluster or a liquid, they are easily carried out. In this model, we assume that, under the conditions of our experiments, most nearest neighbors of the PBN molecule in the argon matrix are argon atoms and only one of the nearest neighbors is an AN molecule. Interactions with AN molecules in the second solvation layer and outer layers are ignored. It is further assumed that, during the deposition process, the PBN/AN pair assumes the most stable conformation of the free cluster in the ground state. The cluster is embedded in an argon matrix using an MD simulation procedure that was described in detail in ref 30. A trapping site containing both PBN and AN is created upon codeposition of the two molecules in an argon matrix. The argon atoms surrounding the site prevent large changes in the relative geometry of the two trapped molecules. It follows that, if the equilibrium geometry of the pair when PBN is in the CT state is similar to that of the pair when PBN is in the ground state, the CT state can attain its equilibrium geometry even in the matrix. However, if the equilibrium geometries of the pair are very different in the two electronic states, the system is constrained to a higher-energy minimum because of the matrix wall effect.[31] Figure 9 shows a schematic presentation of the energy level diagram pertinent to this model.

Support for this qualitative model is provided by calculating the equilibrium structure of a 1:1 PBN/AN cluster in the ground state and in the CT state and comparing the results with similar calculations for a 1:1 PP/AN cluster.

The calculation of the structure of the clusters was carried out using the method described in section II.2.[32] The most stable configuration of PBN (or PP) in its CT state in the presence of AN was calculated by the same procedure: First, the equilibrium geometry of a PBN/AN 1:1 cluster was calculated using the charge distribution of the CT state. The parameters used for the atom−atom pairwise potentials in eq 1 were the same as in the ground state. This approximation is expected to retain the principal differences between the two molecules, even if the results for both in the excited state might be numerically inaccurate. The two possible CT states (quinoid and antiquinoid) used in the Zilberg−Haas model[15] were included in the calculation.

Figure 10 shows the calculated structures of a 1:1 cluster of PP with AN for the ground state and the two CT states. Figure 11 shows a similar calculation for the PBN/AN 1:1 cluster. The calculated properties of the clusters in their respective minima are summarized in Table 4. One of these forms might be the emitting state in the matrix. As Figure 10 shows, the structures of the PP/AN cluster in the ground state and in both CT states are quite similar. The AN molecule is situated roughly parallel to the long axis of the PP molecule, lying approximately next to the central part of PP. The situation for the PBN/AN cluster is entirely different in the ground state: the two molecules are aligned almost head to tail, with the two CN groups next to each other. This is probably due to the large dipole moment of the cyanide group. In the excited CT states, the most stable structures are similar to those of the PP/AN cluster, i.e., the AN molecule is aligned roughly at the center of PBN.

The dramatic change in the emission spectrum of PP in an AN-doped argon matrix compared to a neat one is explained by the stabilization of the CT state by the presence of AN as a neighbor. Only a very small structural change is required for

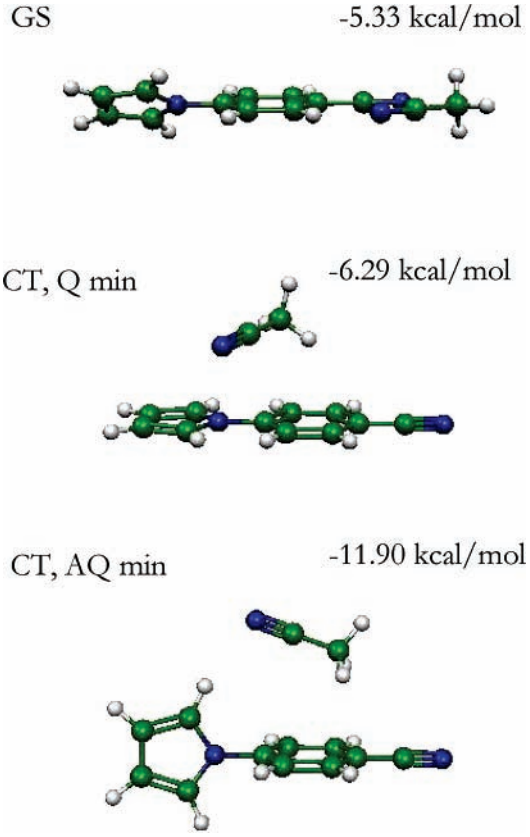

Figure 11. Calculated structures of the most stable 1:1 PBN/AN clusters in the ground state and in the two CT excited states. The energies signify stabilization with respect to the separated molecules.

TABLE 4: Computed CASPT2 Excitation Energies (eV) and Dipole Moments (D) of Some Electronic States of PP and PBN[15]

	PP		PBN	
electronic state	μ (D)	E (ev)	μ (D)	E (ev)
1^1A	−1.3[a]	0	4.1[b]	0
1^1B	0.9-	4.1	4.0	3.8
2^1A(Q)	0.8	4.7	11.0	4.0
2^1A (AQ)	10.8	5.3	16.2[c]	5.1

[a] Negative dipole moments mean direction reversed, from benzene to pyrrol. [b] Experimental value = 3.2 D.[36] [c] Experimental value (in solution) = 22.4 D.[6]

the PP molecule to attain the optimal geometry of the CT state, so that, if the molecule is promoted to this state, a small rearrangement is sufficient to reach the energetically most favorable configuration even though the argon matrix is a rigid medium. The case of PBN is different. In a neat argon matrix, PBN molecules can be excited to the CT state. The presence of an AN neighbor is expected to stabilize the CT state, because of its higher polarity compared to argon. However, as seen from Figure 11, a major structural change is required for the PBN/AN pair to acquire the energetically most favorable configuration in the CT state. Such a transposition necessitates the simultaneous movement of many argon lattice atoms, an unlikely process at the low temperatures prevailing in the matrix. Therefore, the molecule finds itself constrained by the matrix "wall" and cannot achieve complete relaxation.

It should be noted that the small dependence on the excitation wavelength of the PBN emission spectrum in AN-doped argon matrixes is in sharp contrast to the strong dependence in the case of PP.[9] Usually, strong wavelength dependence in rigid environment indicates an inhomogeneous distribution of sites.[33,34] Therefore, the slight dependence observed for PBN can be interpreted as resulting from a rather narrow distribution of sites. Figure 3 shows that, in an argon matrix doped by 1% AN, even excitation at wavelengths longer than the absorption in argon does not lead to a significant red shift of the emission spectrum. This means that in those matrixes, there are no sites (or too few to be detected) whose volume is large enough to enable reorientation of the AN molecule so as to stabilize the CT state. Yet, in argon matrixes doped by higher AN concentrations such as 4.7%, the emission spectrum contains a weak additional band whose maximum is about 410 nm. This added band might arise from sites with more free volume [in which PBN/$(AN)_2$ clusters are trapped] that allow better alignment of AN with respect to PBN through relaxation in the excited state or the second AN is accidentally in the position to which the AN in the cluster would have to move after CT excitation.

IV.4. Different Emission Properties of AN Clusters of PP and PBN in a Supersonic Jet. A remarkable difference between the emission spectra of large PP$(AN)_n$ and PBN$(AN)_n$ clusters ($n \geq 4$) in a supersonic jet was recently reported.[8] Only LE-type fluorescence was observed for these clusters in the case of PP, whereas the PBN clusters exhibited both LE- and CT-type emissions. The structures of these clusters were calculated using the method described in section II.2. As an example, the structures of the most stable PP$(AN)_4$ and PBN$(AN)_4$ in the ground state are shown in Figure 12. In both cases, the four AN molecules are found on the same side of the pyrrol molecule. Inspection of these structures reveals that in the PP$(AN)_4$ cluster the structure of the $(AN)_4$ fragment is practically the same as that of an isolated cluster of four AN molecules.[35] This reflects the fact that the bonding between two AN molecules is stronger than the AN−PP bond, probably because of a strong dipole−dipole interaction. In sharp contrast, the structure of the PBN-$(AN)_4$ cluster is completely different: there is no similarity between the $(AN)_4$ fragment and an isolated one. This difference is due to the higher dipole moment of PBN (compared to PP) and to the interaction between the cyano gropu of PBN with the AN molecule.

Electronic excitation of the PP$(AN)_{n\geq4}$ cluster leads to initial population of the LE state. If the excess energy deposited in the cluster exceeds the PP−AN bond dissociation energy, the most likely result is dissociation of this bond. In the case of the PBN$(AN)_{n\geq4}$ clusters, the binding is stronger, and the rate of intramolecular CT to form the CT state might exceed the rate of cluster dissociation. Furthermore, as shown in ref 8, the CT state can be directly excited in this case by UV absorption.

IV.5. Emission Spectra of PBN in Xenon and CO_2 Matrixes. The structure of the emission spectrum recorded in Xe and CO_2 (Figure 4) resembles that of the spectrum recorded in AN-doped argon matrixes: only a broad and structureless emission band is observed. This suggests that, in these matrixes, as in argon/AN matrixes, emission results only from the CT state. The fluorescence signal recorded from PBN in xenon was weaker by about an order of magnitude than the signal recorded in argon or CO_2, most likely because of the higher ISC rate in that medium. It can be seen from Figure 4 that increasing the polarizability of the matrix material (from Ar to CO_2 and Xe) leads to a red shift of the fluorescence spectrum. This shift can be explained by a better stabilization of the PBN CT state by solute-induced dipole interaction. The dependence of the emission maximum on the polarizability of the medium can be regarded as further support for the assignment proposed as such a large solvent influence on emission is observed only for polar excited states. The discrete bands assignable to the $1A(S_0)$−

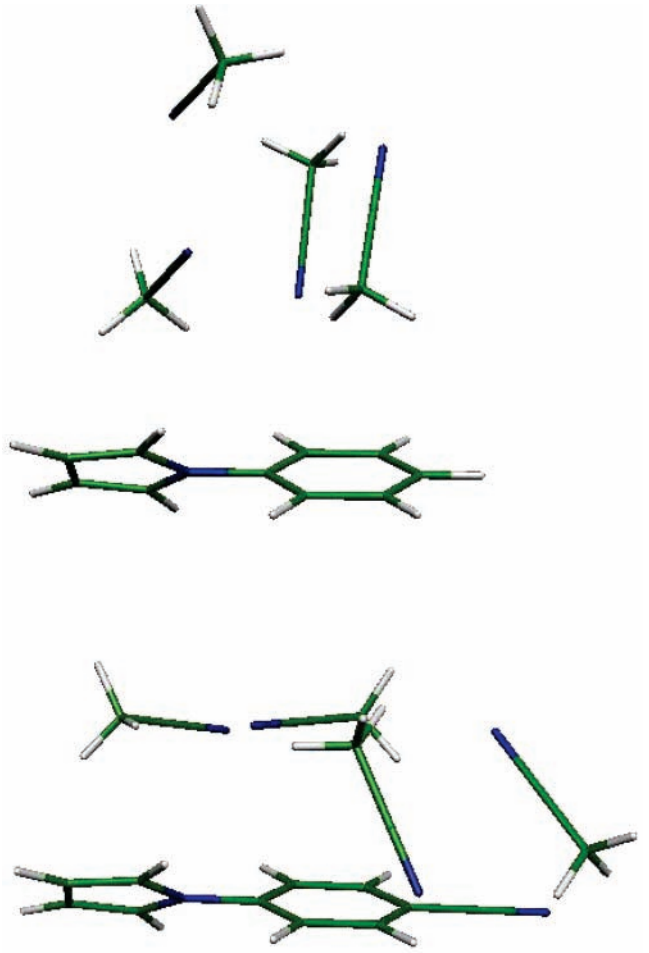

Figure 12. Calculated structures of the most stable PP/$(AN)_4$ cluster (left) and the most stable PBN/$(AN)_4$ cluster (right) in their respective ground states. Note that the structure of the $(AN)_4$ moiety in the case of the PP adduct is essentially identical to that of a free $(AN)_4$ cluster whereas in the case of the PBN cluster, it is distorted from that of the free cluster. (Numerical values are given in Figure S2 in the Supporting Information.)

1B(LE) transition (Figure 7) are not observed in these matrixes. This might indicate a more rapid depletion of the initially excited LE state as a result of either the enhanced ISC in the xenon matrix or the CT state, which is lower-lying (with respect to the LE state) than in an argon matrix. It is interesting to notice that the emission in xenon is broader (by $\sim$1500 cm^{-1}) than that in the two other media. A possible explanation for this broadened emission is that the xenon atoms surrounding the PBN molecule stabilize the two CT minima to the extent that both become lower than the excitation energy. Therefore, the emission spectrum is composed of two bands, arising from two different CT minima.

V. Summary

The main results of this work can be summarized as follows:

(1) The LE emission spectrum (due to the B−X transition) of PP in an argon matrix is red-shifted with respect to the gas phase, whereas that of PBN it is blue-shifted. This indicates that the B state of PP is more polar than the ground state whereas, in the case of PBN, it is less polar.

(2) The global minimum of the CT state in an argon matrix is lower in energy than the LE state and can be directly excited by light absorption.

(3) Addition of acetonitrile to the argon matrix containing PP leads to the appearance of a well-separated emission band due to the CT state, whereas in the case of PBN, the spectral shift is much smaller. Addition of AN to an argon matrix reverses the order of the LE (B) and CT levels in the case of PP, hence producing a large change, whereas for PBN, the CT level is lowest in both cases, yielding only small additional shift due to AN. These results are explained by the different structures of the pyrrol/acetonitrile 1:1 adduct: in the case of PP, the equilibrium structure of the adduct is similar in the ground and CT states, whereas in the case of PBN, they are dramatically different. It follows that a large-amplitude motion of the AN cosolvent molecule is required in the case of PBN to reach the equilibrium geometry of the PBN/AN pair. The argon matrix cage does not permit large-amplitude motions, so that the emission is from a strained adduct, shifted to the blue with respect to the spectrum in fluid systems in which this motion is allowed.

(4) The demonstration of direct CT-state excitation of PBN in an argon matrix might indicate that, in the case of this molecule, this state can be populated by direct light absorption in other solvents as well, in addition to its population by a nonradiative process from the LE state.

Acknowledgment. We thank Dr. S. Zilberg, Dr. W. Fuss, and Dr. K. Zachariasse for many helpful discussions. We are grateful to Dr. Zachariasse for making ref 25 available to us prior to publication. This research was supported by the Israel Science Foundation and by The Volkswagen-Stiftung (I/76 283). The Farkas Center for Light Induced Processes is supported by the Minerva Gesellschaft mbH.

Supporting Information Available: Parameters used in simulation, detailed view of blue part of emission spectrum of PN in an argon matrix, numerical values for Figure 12, and calculated charges for PP and PBN in the ground and two CT states. This material is available free of charge via the Internet at http://pubs.acs.org.

References and Notes

(1) Grabowski, Z. R.; Rotkiewicz, K.; Rettig, W. *Chem. Rev.* **2003**, *103*, 3899.

(2) Rettig, W.; Marschner, F. *Nouv. J. Chim.* **1983**, *7*, 425.

(3) PP and PBN as well as most other molecules derived from aminobenzene, have a C_2 symmetry axis and belong to either the C_2 or C_{2v} point group. The ground state has A (or A_1) symmetry; the first excited state, B (or B_2) symmetry; and the second excited state, A (or A_1) symmetry. The CT state is derived from the 2A state. It is customary to label the 1^1B state as the LE state (or B state) and the 2^1A state as the CT state (or A state). Another CT state with B symmetry is also predicted by some quantum chemical calculations (ref 23).

(4) Sarkar, A.; Chakravorti, S. *Chem. Phys. Lett.* **1995**, *235*, 195.

(5) Yoshihara, T.; Galievski, V. A.; Druzhinin,. I. S.; Saha, S.; Zachariasse, K. A. *Photochem. Photobiol. Sci.* **2003**, *2*, 342.

(6) Cornelissen-Gude, C.; Rettig, W. *J. Phys. Chem. A* **1998**, *102*, 7754.

(7) Belau, L.; Haas, Y. *Chem. Phys. Lett.* **2002**, *364*, 157.

(8) Belau, L.; Haas, Y.; Rettig, W. *J. Phys. Chem. A* **2004**, *108*, 3916.

(9) Schweke, D.; Haas, Y. *J. Phys. Chem. A* **2003**, 107.

(10) Rettig, W.; Marschner, F. *New J. Chem.* **1990**, *14*, 819.

(11) Jorgensen, W. L.; Briggs, J. M. *Mol. Phys.* **1988**, *63*, 547.

(12) McDonald, N. A.; Jorgensen, W. L. *J. Phys. Chem. B* **1998**, *102*, 8049.

(13) Jorgensen, W. L.; Laird, E. R.; Nguyen, T. B.; Tirado-Rives, J. *J. Comput. Chem.* **1993**, *14*, 206.

(14) Bohm, H. J.; McDonald, I. R.; Maden, P. A. *Mol. Phys.* **1983**, *49*, 347.

(15) Zilberg, S.; Haas, Y. *J. Phys. Chem. A* **2002**, *104*, 1.

(16) Singh, U. C.; Kollman, P. A. *J. Comput. Chem.* **1984**, *5*, 129. Besler, B. H.; Merz, K. M., Jr.; Kollman, P. A. *J. Comput. Chem.* **1990**, *11*, 431.

(17) Nelder, J. A.; Mead, R. *Comput. J.* **1965**, *7*, 308.

(18) Powell, M. J. D. *Comput. J.* **1964**, *7*, 155.
(19) Powell, M. J. D. *Lecture Notes in Mathematics*; Vol. 1066; Springer: New York, 1984; pp 122−141. See also: http://math.fullerton.edu/mathews/n2003/PowellMethodMod.html.
(20) Old Powell: Press, W. H.; Teukolsky, S. A.; Vetterling, W. T.; Flannery, B. P. *Numerical Recipes in FORTRAN, the Art of Scientific Computing*; Cambridge University Press: Cambridge, U.K., 1992; p 387ff. (b) New Powell: Powell, M. J. D. *Optimization Methods and Software, Program NEWUOA*; Report No. DAMTP 2003/NA03; University of Cambridge: Cambridge, U.K., 2003.
(21) Schweke, D.; Haas, Y.; Dick, B., submitted to J. Phys. Chem. A.
(22) In Table 3, the very weak band at 35463 cm^{-1} is not included. It might be due to still another trapping site, but the S/N ratio is not sufficient for a firm analysis.
(23) Parusel, A. B. *Phys. Chem. Chem. Phys.* **2000**, *2*, 5545.
(24) Demeter, A.; Druzhinin, S.; George, M.; Haselbach, E.; Roulin, J.-L.; Zachariasse, K. A. *Chem. Phys. Lett.* **2000**, *323*, 351.
(25) Yoshihara, T.; Druzhinin, S. I.; Demeter, A.; Kocher, N.; Stalke, D.; Zachariasse, K. A. *J. Phys. Chem. A*, in press.
(26) Il'ichev, Yu. V.; Kühnle, W.; Zachariasse, K. A. *J. Phys. Chem. A* **1998**, *102*, 5670.
(27) Rotkiewicz, K.; Grellman, K. H.; Grabowski, Z. R. *Chem. Phys. Lett.* **1973**, *19*, 315.
(28) Zachariasse, K. A.; Grobys, M.; von der Haar, Th.; Hebecker, A.; Ilichev, Yu. V.; Jiang, Y.-B.; Morawski, O.; Kühnle, W. *J. Photochem. Photobiol. A: Chem.* **1996**, *102*, 59.
(29) Fuss, W.; Pushpa, K. K.; Rettig, W.; Schmid, W. E.; Trushin, S. A. *Photochem. Photobiol. Sci.* **2002**, *1*, 256. Yatsuhashi, T.; Trushin, S. A.; Fuss, W.; Rettig, W.; Schmid, W. E.; Zilberg, S. *Chem. Phys.* **2004**, *296*, 1.
(30) Fraenkel, R.; Haas, Y. *Chem. Phys.* **1994**, *186*, 185; Fraenkel, R.; Schweke, D.; Haas, Y.; Molnar, F.; Horinek, D.; Dick, B. *J. Phys. Chem. A* **2000**, *104*, 3786.
(31) Kasha, M.; Sytnik, A.; Dellinger, B. *Pure Appl. Chem.* **1993**, *65*, 1641.
(32) The calculated charges are shown in Figures S3 (PP) and S4 (PBN) in the Supporting Information.
(33) Haas, Y.; Samuni, U. *Prog. React. Kinet.* **1998**, *23*, 211.
(34) Al-Hassan, K. A.; Rettig, W. *Chem. Phys. Lett.* **1986**, *126*, 273.
(35) Siebers, J. G.; Buck, U.; Beu, T. A. *Chem. Phys.* **1998**, *239*, 549.
(36) Lumbroso, H.; Bertin, D. M.; Marschner, F. *J. Mol. Struct.* **1988**, *178*, 187.